

# Stochastic gravitational wave background from the collisions of dark matter halos

Qiming Yan<sup>a,1,2,3,4</sup>, Xin Ren<sup>b,1,2</sup>, Yaqi Zhao<sup>c,1,2</sup>, Emmanuel N. Saridakis<sup>d,5,1,2,6</sup>

<sup>1</sup>Deep Space Exploration Laboratory/School of Physical Sciences, University of Science and Technology of China, Hefei, Anhui 230026, China

<sup>2</sup>CAS Key Laboratory for Researches in Galaxies and Cosmology/Department of Astronomy, School of Astronomy and Space Science, University of Science and Technology of China, Hefei, Anhui 230026, China

<sup>3</sup>School of Astronomy and Space Science, University of Chinese Academy of Sciences, Beijing 100049, China

<sup>4</sup>Kavli Institute for Astronomy and Astrophysics, and School of Physics, Peking University, Beijing, 100871, China

<sup>5</sup>National Observatory of Athens, Lofos Nymfon, 11852 Athens, Greece

<sup>6</sup>Departamento de Matemáticas, Universidad Católica del Norte, Avda. Angamos 0610, Casilla 1280 Antofagasta, Chile

Received: date / Accepted: date

**Abstract** We investigate the effect of the dark matter (DM) halos collisions, namely collisions of galaxies and galaxy clusters, through gravitational bremsstrahlung, on the stochastic gravitational wave background. We first calculate the gravitational wave signal of a single collision event, assuming point masses and linear perturbation theory. Then we proceed to the calculation of the energy spectrum of the collective effect of all dark matter collisions in the Universe. Concerning the DM halo collision rate, we show that it is given by the product of the number density of DM halos, which is calculated by the extended Press-Schechter (EPS) theory, with the collision rate of a single DM halo, which is given by simulation results, with a function of the linear growth rate of matter density through cosmological evolution. Hence, integrating over all mass and distance ranges, we finally extract the spectrum of the stochastic gravitational wave background created by DM halos collisions. As we show, the resulting contribution to the stochastic gravitational wave background is of the order of  $h_c \approx 10^{-29}$  in the band of  $f \approx 10^{-15} Hz$ . However, in very low frequency band, it is larger. With current observational sensitivity it cannot be detected.

**Keywords** Stochastic gravitational wave · gravitational wave source · pulsar time array

## 1 Introduction

Recently, the gravitational wave (GW) detecting technology has been developing rapidly. In 2015, the detection

of binary black holes merger GW150914 by the LIGO experimental cooperation signaled the first detection of gravitational waves [1], while in 2017, the joint detection of GW170817 [2] and GRB170817A [3] opened the new era of multi-messenger astronomy [4]. In general, with the increasing amount of detected gravitational wave events [5] one has improved statistics that allows to track the history of the universe [6,7] and impose bounds on various cosmological parameters [8,9], as well as constrain various theories of gravity [10,11,12,13,14]. Moreover, for different frequencies and types of gravitational wave sources, various detection means have been designed and implemented. Besides ground-based laser interferometers such as LIGO, Virgo and KAGRA, which probe high frequency bands ( $10 - 10^4$  Hz), space-based laser interferometers such as LISA [15,16,17,18] for intermediate frequency gravitational waves ( $10^{-4} - 1$  Hz), and the pulsar timing array (PTA) [19,20,21,22,23,24] for lower frequency bands ( $10^{-9} - 10^{-6}$  Hz), are also raised. These observational avenues allow us to acquire rich information from GWs of different types and sources, among which stochastic gravitational wave background is attracting increasing interest.

Stochastic gravitational wave background (GWB) is a type of random background signal that exists in an analogous way to the cosmic microwave background. The contribution of GWB can be roughly divided into cosmological sources and astrophysical sources [25]. Astrophysical originated GWB contains all types of unresolved GW emitting events, including binary black hole mergers [26,27,28,29,30,31,32]. These signals can provide information about astrophysical source populations and processes over the history of the universe [33,34,35,36]. On the other hand, cosmological originated GWB mainly involves primordial gravitational perturba-

<sup>a</sup>e-mail: yqmtobephd@stu.pku.edu.cn

<sup>b</sup>e-mail: rx76@ustc.edu.cn

<sup>c</sup>e-mail: zxmyg86400@mail.ustc.edu.cn

<sup>d</sup>e-mail: msaridak@noa.gr

tions during the inflation epoch [37, 38, 39], or perturbations arising from primordial black holes fluctuations [40, 41, 42, 43, 44]. GW signals typically remain unaffected during their propagation, and thus they can provide valuable information about the very early stages of the universe. For instance, different inflationary models can lead to different predictions for the GWB spectrum [45, 46, 47, 48, 49, 50, 51, 52, 53, 54, 55, 56, 57], and thus GWB can be used as a probe of this primordial universe epoch. Since GWB can provide us with important astrophysical and cosmological probes, it is crucial to understand its composition and properties [58, 59, 60, 61, 62, 63, 64, 65, 66, 67, 68, 69].

On the other hand, according to observations, dark matter (DM) constitutes a significant fraction of the energy density of the universe [70, 71, 72]. Its microphysical nature and possible interactions remain unknown [73, 74, 75, 76], nevertheless we do know unambiguously that DM takes part in gravitational interaction [77, 78]. Current theory predicts that the main part of DM is concentrated in dark halos, which coincide in position with galaxy or galaxy clusters [79]. These galaxies and galaxy clusters, and thus dark halos too, are typically accelerating and merging through their mutual attraction [80, 81, 82]. Such processes can in principle release GW signal through gravitational bremsstrahlung [83, 84, 85, 86, 87, 88, 89, 90, 91, 92, 93, 94, 95]. This process can be approximately described as an elastic collision between two particles. The approximate calculation results of the gravitational waves released during the collision process have been obtained previously in some literature [96]. However, it is important to note that simply considering the gravitational waves released during the elastic collision process is the ideal hypothesis because the release of gravitational waves takes away the system's energy, making the collision no longer elastic. Therefore, the gravitational wave spectrum calculated in this way can only be applicable below a certain cutoff frequency.

In this work, we are interested in investigating for the first time the possible GW signals that could be emitted through bremsstrahlung during dark halo merger and collisions, and their contribution to the stochastic GWB. In particular, we will first consider a single event of two DM halos collision, and we will calculate the emitted GW signal. Then, we will calculate the energy spectrum contribution to the stochastic GWB, taking the DM halo collision rate into consideration. The structure of the article is as follows. In Section 2 we analyze the GW emitted during the collision of two galaxies or two galaxy clusters. In Section 3 we integrate over redshift and DM halos parameters to extract the contribution to stochastic GWB. Finally, in Section 4 we conclude and discuss our results.

## 2 Gravitational waves emitted during a single collision

In this section, we aim at estimating the gravitational waves emitted during a single collision event. In particular, we calculate the GW radiated by the collision of two DM halos, which corresponds to the collision of two galaxies or two galaxy clusters.

[96] considered the gravitational waves released during the elastic collision between two particles. In section 4.4.1 of [96], the energy-momentum tensor was approximated directly using the 4-momentum of the particles before and after the collision without considering collision process.

In the case where the collision velocity is much lower than the speed of light  $c$ , let A and B be the two particles participating in the collision,  $m_Q$ ,  $p_Q^\mu$ ,  $p'_Q{}^\mu$  and  $\vec{v}_Q$ ,  $\vec{v}'_Q$  be the mass, 4-momenta and velocities of particle Q before and after the collision. Then, before the collision occurs, the energy-momentum tensor of the two particles is given by  $\sum_{Q=A,B} \frac{p_Q^\mu p_Q^\nu}{m_Q} \delta^{(3)}(\vec{x}_Q - \vec{v}_Q t)$ . Treating the collision process as instantaneous, the collision occurs at  $t = 0$ . Afterwards, the energy-momentum tensor of the two particles is given by  $\sum_{Q=A,B} \frac{p'_Q{}^\mu p'_Q{}^\nu}{m_Q} \delta^{(3)}(\vec{x}_Q - \vec{v}'_Q t)$ . Let  $\theta(t)$  be the unit step function. In this way, the energy-momentum tensor of the particles throughout the entire process can be written as

$$T^{\mu\nu} \approx \sum_{Q=A,B} \frac{p_Q^\mu p_Q^\nu}{m_Q} \delta^{(3)}(\vec{x}_Q - \vec{v}_Q t) \theta(-t) + \frac{p'_Q{}^\mu p'_Q{}^\nu}{m_Q} \delta^{(3)}(\vec{x}_Q - \vec{v}'_Q t) \theta(t). \quad (1)$$

Based on this energy-momentum tensor, the gravitational wave energy spectrum can be further calculated. In the next section, we will see the energy spectrum given in this article is consistent with that in [96] at relatively high frequencies. However, since we give the precise calculation of the particle motion during the entire collision process, in our calculation we also give the contribution of the lower-frequency gravitational waves compared to the results given in [96].

Besides, at very high frequencies, the physical processes corresponding to the emission of high-frequency gravitational waves are not reflected in either analytical method and cannot be dealt with. As a result, the gravitational wave spectra obtained from both methods can only be applicable below a certain cut-off frequency. In fact, without using numerical relativity for high precision calculations, any gravitational wave spectra obtained through analytical methods require an artificially estimated cut-off frequency. In the next section, we will see that the spectra obtained from both methods diverge

when integrated to arbitrarily high frequencies, thus necessitating the establishment of a cut-off frequency.

The following is a more detailed and accurate calculation process we carried out. According to observations, such a collision typically has a huge duration, which in turn implies that the energy radiated through GWs per unit time is not very large, and thus we can safely use linear perturbation theory in the involved calculations. Specifically, we use [97]

$$g_{\mu\nu} = \eta_{\mu\nu} + h_{\mu\nu}, \quad |h_{\mu\nu}| \ll 1, \quad (2)$$

$$\bar{h}_{ij}(t, \mathbf{x}) = \frac{2G}{rc^4} \frac{d^2 I_{ij}(t_r)}{dt^2}, \quad t_r = t - \frac{r}{c}, \quad (3)$$

where  $G$  is the gravitational constant,  $c$  is the speed of light, and  $r$  is the distance from us to the center of mass of the two galaxies or galaxy clusters. Moreover,  $I_{ij}$  is the quadrupole moment

$$I_{ij}(t) = \int y^i y^j T^{00}(t, \mathbf{y}) d^3 y = \int y^i y^j \rho(t, \mathbf{y}) d^3 y, \quad (4)$$

where  $T^{\mu\nu}$  is energy-momentum tensor,  $\rho$  is energy density, and  $y^i$  is the spatial coordinate. Since the goal of our calculation is to acquire an estimation of the order of the magnitude of the resulting signal, we can consider these two DM halos as mass points, with mass  $M_a$  and position  $\mathbf{y}_{(a)}(t)$  at time  $t$ . Hence, the density  $\rho$  can be written as

$$\rho(t, \mathbf{y}) = \sum_a M_a \delta^3(\mathbf{y} - \mathbf{y}_{(a)}(t)), \quad (5)$$

while the quadrupole moment  $I_{ij}(t)$  becomes

$$I_{ij}(t) = \int y^i y^j \rho(t, \mathbf{y}) d^3 y = \sum_a M_a y_{(a)}^i(t) y_{(a)}^j(t). \quad (6)$$

Finally, since the relative speed of two galaxies or galaxy clusters is much smaller than the speed of light, we can use Newtonian mechanics to handle their dynamics.

For simplicity, we write the equations in the center-of-mass frame of these two mass points. By definition, we have

$$M_A \mathbf{r}_A + M_B \mathbf{r}_B = \mathbf{0}, \quad (7)$$

where  $M_A$ ,  $M_B$  are the masses of the mass points A and B, with  $\mathbf{r}_A$ ,  $\mathbf{r}_B$  their position vectors. From Newtonian mechanics we have

$$\ddot{\mathbf{r}}_A = -\frac{GM_B}{|\mathbf{r}_A - \mathbf{r}_B|^2} \frac{\mathbf{r}_A}{|\mathbf{r}_A|}, \quad (8)$$

which using (7) gives

$$\ddot{\mathbf{r}}_A = -\mu_B \frac{\mathbf{r}_A}{|\mathbf{r}_A|^3}, \quad (9)$$

where we have defined  $\mu_B \equiv \frac{GM_B}{(1 + \frac{M_B}{M_A})^2}$ . Additionally, we assume that the two points are initially at infinite distance, their relative speed is  $v_\infty = v_{A\infty} + v_{B\infty}$ , and the impact parameter is  $b = b_A + b_B$ . From Newtonian mechanics we know that the trajectory of each point is a hyperbola and the two points are moving in a plane (we set this plane as  $z = 0$  plane, and thus  $\mathbf{r}_A = (x_A, y_A, 0)$ ), while the total energy of the system is positive. Additionally, the mass center of these two DM halos will not follow a hyperbolic trajectory at all times, in order to acquire a collision. In Fig. 1 we depict an illustrative representation of the initial conditions of the collision.

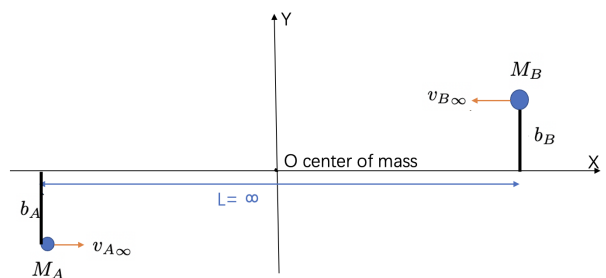


**Fig. 1** An illustrative representation of the initial conditions of the collision. The two galaxies or galaxy clusters are considered as points with masses  $M_A$  and  $M_B$ , where  $b_A$  and  $b_B$  are the impact parameters.

Let us start with the beginning of the collision, when the two DM halos start moving towards each other. For point A we have

$$(x_A + a_A e_A)^2 - (y_A)^2 = a_A^2, \quad (10)$$

where

$$a_A = \frac{\mu_B}{(v_{A\infty})^2}, \quad (11)$$

$$e_A = \sqrt{1 + \frac{v_{A\infty}^4 b_A^2}{(\mu_B)^2}}, \quad (12)$$

$$a = a_A + a_B. \quad (13)$$

We proceed by defining  $\lambda_A$  through

$$e_A \sinh(\lambda_A) - \lambda_A = \frac{v_{A\infty} t}{a_A}, \quad (14)$$

hence

$$r_A^1 = x_A = a_A [e_A - \cosh(\lambda_A)], \quad (15)$$

$$r_A^2 = y_A = a_A \left[ \sqrt{e_A^2 - 1} \sinh(\lambda_A) \right]. \quad (16)$$

Note that  $t = 0$  corresponds to the time when the two mass points have the shortest distance.

In order to obtain the GW amplitude  $h_{ij}$ , we proceed to the calculation of the quadrupole moment  $I_{ij}(t)$  and its second time derivative. We have

$$I_{ij} = M_A r_A^i r_A^j + M_B r_B^i r_B^j, \quad (17)$$

$$\begin{aligned} \frac{d^2 I_{ij}}{dt^2} &= M_A (\ddot{r}_A^i r_A^j + \dot{r}_A^i \dot{r}_A^j + 2\dot{r}_A^i \dot{r}_A^j) \\ &+ M_B (\ddot{r}_B^i r_B^j + \dot{r}_B^i \dot{r}_B^j + 2\dot{r}_B^i \dot{r}_B^j). \end{aligned} \quad (18)$$

From (15), (16) we find

$$\dot{x}_A = -\frac{a_A \sinh(\lambda_A)}{\sqrt{\frac{a_A^3}{\mu_B} [e_A \cosh(\lambda_A) - 1]}}, \quad (19)$$

$$\ddot{x}_A = \frac{\mu_B (\cosh(\lambda_A) - e)}{a_A^2 [e_A \cosh(\lambda_A) - 1]^3}, \quad (20)$$

$$\dot{y}_A = \frac{a_A \sqrt{e_A^2 - 1} \cosh(\lambda_A)}{\sqrt{\frac{a_A^3}{\mu_B} [e_A \cosh(\lambda_A) - 1]}}, \quad (21)$$

$$\ddot{y}_A = -\frac{\sqrt{e_A^2 - 1} \mu_B \sinh(\lambda_A)}{a_A^2 [e_A \cosh(\lambda_A) - 1]^3}, \quad (22)$$

and thus inserting into (18) we extract all the second time derivatives of the quadrupole moment  $I_{ij}(t)$ , namely

$$\begin{aligned} \frac{d^2 I_{11}}{dt^2} &= \frac{\mu_B M_A}{2a_A [e_A \cosh(\lambda_A) - 1]^3} \\ &\times \{7e_A \cosh(\lambda_A) + e_A [\cosh(3\lambda_A) - 4e_A] - 4 \cosh(2\lambda_A)\} \\ &+ \frac{\mu_A M_B}{2a_B [e_B \cosh(\lambda_B) - 1]^3} \\ &\times \{7e_B \cosh(\lambda_B) + e_B [\cosh(3\lambda_B) - 4e_B] - 4 \cosh(2\lambda_B)\}, \end{aligned} \quad (23)$$

$$\begin{aligned} \frac{d^2 I_{12}}{dt^2} &= -\frac{\sqrt{e_A^2 - 1} \mu_B M_A \sinh(\lambda_A)}{a_A [e_A \cosh(\lambda_A) - 1]^3} \\ &\times \{e_A [\cosh(2\lambda_A) + 3] - 4 \cosh(\lambda_A)\} \\ &- \frac{\sqrt{e_B^2 - 1} \mu_B M_A \sinh(\lambda_B)}{a_B [e_B \cosh(\lambda_B) - 1]^3} \\ &\times \{e_B [\cosh(2\lambda_B) + 3] - 4 \cosh(\lambda_B)\}, \end{aligned} \quad (24)$$

$$\begin{aligned} \frac{d^2 I_{22}}{dt^2} &= \frac{(e_A^2 - 1) \mu_B M_A}{2a_A [e_A \cosh(\lambda_A) - 1]^3} \\ &\times [3e_A \cosh(\lambda_A) + e_A \cosh(3\lambda_A) - 4 \cosh(2\lambda_A)] \\ &+ \frac{(e_B^2 - 1) \mu_A M_B}{2a_B [e_B \cosh(\lambda_B) - 1]^3} \\ &\times [3e_B \cosh(\lambda_B) + e_B \cosh(3\lambda_B) - 4 \cosh(2\lambda_B)]. \end{aligned} \quad (25)$$

For simplicity, we define  $M \equiv M_A + M_B$ , and the mass ratio  $x \equiv M_A/M_B$ . Noting that we have  $M_A b_A = M_B b_B$  and  $M_A v_{A\infty} = M_B v_{B\infty}$ , so that  $1/x = b_A/b_B = v_{A\infty}/v_{B\infty}$ .

As a result, we get  $M_A = \frac{M}{(1+1/x)}$ ,  $M_B = \frac{M}{1+x}$ ,  $b_A = \frac{b}{1+x}$ ,  $b_B = \frac{b}{1+1/x}$ ,  $v_{A\infty} = \frac{v_\infty}{1+x}$ ,  $v_{B\infty} = \frac{v_\infty}{1+1/x}$ . Substitute the above equations into the formula of  $\mu_B, a_A, e_A$ , we

have

$$\mu_B = \frac{GM}{(1+x)^3} \quad (26)$$

$$a_A = \frac{GM}{v_\infty^2} \frac{1}{1+x} \quad (27)$$

$$e_A = \sqrt{1 + \left(\frac{bv_\infty^2}{GM}\right)^2} \quad (28)$$

We note that  $e_A$  is independent from mass ratio  $x$ , so  $e_A = e_B$ . Besides,  $v_{A\infty}/a_A = v_\infty^3/GM$  is also independent from mass ratio  $x$ , so the  $\lambda_A$  is just equal to  $\lambda_B$ . In short, the mass ratio  $x$  only affects  $\ddot{I}_{ij}$  by factors like  $\mu_B M_A/a_A = Mv_\infty^2 x/(1+x)^3$ . Therefore, we can get the results in any mass ratio from the equal mass result by the following equation,

$$\ddot{I}_{ij}(M, x) = 4 \left[ \frac{x}{(1+x)^3} + \frac{1/x}{(1+1/x)^3} \right] \ddot{I}_{ij}(M, x=1) \quad (29)$$

We can now use (3) in order to obtain the GW signal in the time domain. As typical values we set  $M_A = M_B = 10^9 M_\odot$ , namely the order of mass of a (dwarf) galaxy, where  $M_\odot$  is the mass of the Sun, and we use  $v_{A\infty} = v_{B\infty} = 300 \text{ km/s}$ ,  $b_A = b_B = 10^4 \text{ ly}$ , which are the typical values for galaxy collisions. Moreover, we assume that the collision happens at a distance of  $10^9 \text{ ly}$  from the Earth, which is roughly the distance of the source of GW150914. Hence, we can estimate the magnitude of the GW signal. In Fig. 2 we present the obtained dimensionless GW signal  $\bar{h}_{ij}$ , as a function of time  $t$ . Since  $t = 0$  corresponds to the time of shortest distance, the change rate of  $\bar{h}_{ij}$  is fastest at this time, as expected. As we observe, the variation of  $\bar{h}_{ij}$  is of the order of  $5 \times 10^{-22}$  during the collision. However, this variation corresponds to a large time scale (about  $10^{15} \text{ s}$ ), which implies that a single signal of this kind of GW is extremely hard to be detected. Additionally, we can see that the evolution of  $\bar{h}_{12}$  is faster than that of  $\bar{h}_{11}$ ,  $\bar{h}_{22}$ , which implies that  $\bar{h}_{12}$  will be dominant in relatively higher frequency than that of  $\bar{h}_{11}$ ,  $\bar{h}_{22}$ .

The GW amplitude in TT gauge  $h^{TT}$  is the traceless version of  $\bar{h}_{ij}$ . We can project the GW amplitude in TT gauge by

$$h_{11}^{TT} = \frac{2}{3} \bar{h}_{11} - \frac{1}{3} \bar{h}_{22}, \quad (30)$$

$$h_{22}^{TT} = -\frac{1}{3} \bar{h}_{11} + \frac{2}{3} \bar{h}_{22}, \quad (31)$$

$$h_{33}^{TT} = -\frac{1}{3} \bar{h}_{11} - \frac{1}{3} \bar{h}_{22}, \quad (32)$$

$$h_{21}^{TT} = h_{12}^{TT} = \bar{h}_{12}, \quad (33)$$

while all other  $h_{ij}^{TT}$  are equal to zero.

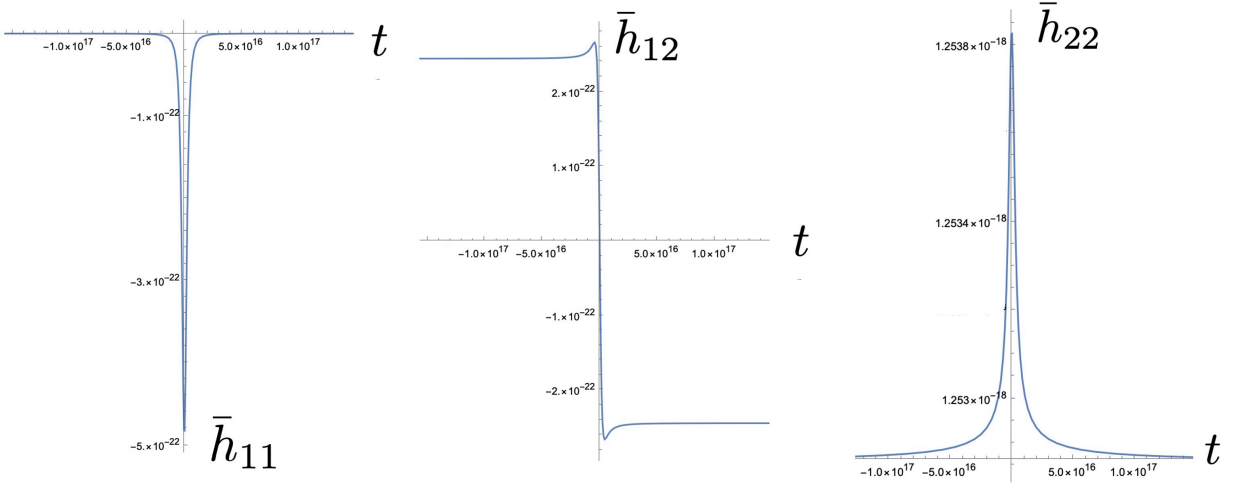


**Fig. 2** The dimensionless components of the gravitational wave signal arising from a single event of the collision of two DM halos, i.e., the collision of two galaxies or clusters of galaxies. The left panel shows the  $\bar{h}_{11}$  component, the middle panel the  $\bar{h}_{12}$  component and the right panel the  $\bar{h}_{22}$  component. The time  $t = 0$  corresponds to the shortest distance between the two DM halos, that is the moment in which  $\bar{h}_{11}$  and  $\bar{h}_{22}$  reach their peaks and  $\bar{h}_{12}$  exhibits the largest variation. We have imposed the typical values  $M_A = M_B = 10^9 M_\odot$ ,  $v_{A\infty} = v_{B\infty} = 300 \text{ km/s}$ ,  $b_A = b_B = 10^4 \text{ ly}$ , and we have assumed that the distance from Earth is  $\sim 10^9 \text{ ly}$ . Time  $t$  is measured in seconds.

We proceed by taking the Fourier transformation of  $\bar{h}_{ij}, h_{ij}^{TT}$ , in order to investigate its spectrum. In particular, we use

$$\tilde{\bar{h}}_{ij}(\omega) = \int_{t=-\infty}^{t=+\infty} dt e^{i\omega t} \bar{h}_{ij}(t), \quad (34)$$

$$\tilde{h}_{ij}^{TT}(\omega) = \int_{t=-\infty}^{t=+\infty} dt e^{i\omega t} h_{ij}^{TT}(t) \quad (35)$$

where  $\omega = 2\pi f$ , with  $f$  the frequency.  $\tilde{\bar{h}}_{ij}(f)$  obey the power law in a very good approximation for a very wide frequency range. Besides, as  $\tilde{\bar{h}}_{11}, \tilde{\bar{h}}_{22} \propto 1/f^2$ , while  $\tilde{\bar{h}}_{12} \propto 1/f$ , we can infer that  $\tilde{\bar{h}}_{11}, \tilde{\bar{h}}_{22}$  will be dominant in the low frequency band while  $\tilde{\bar{h}}_{12}$  will be dominant in relatively high frequencies. In Fig. 3 we present the dependence of  $\tilde{h}_{ij}^{TT}(\omega)(f)$  on  $f$ .

### 3 Effect on the stochastic gravitational wave background

In this section, we calculate the contribution of the DM halos collisions to the stochastic gravitational wave background. Specifically, we integrate the gravitational wave spectrum of a single collision event over the number density of GW sources.

In principle, in order to compare a theoretical model with observations, one uses both the fractional energy density spectrum  $\Omega_{gw}(f)$ , as well as the characteristic

strain amplitude  $h_c(f)$  [61]. They are related to the energy spectrum of GWB through the expression

$$\frac{\pi c^2}{4G} f^2 h_c^2(f) = \rho_c \Omega_{gw}(f) = \frac{d\rho_{gw}(f)}{d \ln f}. \quad (36)$$

where  $f$  is the frequency of GW detected on Earth, and  $\rho_c \equiv 3c^2 H_0^2 / 8\pi G$  is the critical energy density. The energy spectrum of the stochastic GWB,  $\frac{d\rho_{gw}}{d \ln f}$ , can be written as

$$\frac{d\rho_{gw}(f)}{d \ln f} = \int_0^\infty dz \frac{1}{1+z} \int d\xi \frac{dn}{dz d\xi} \frac{dE(\xi)_{gw}}{d \ln f_r} \Big|_{f_r=f(1+z)}, \quad (37)$$

with  $z$  the redshift at the GW emission. Additionally,  $\frac{dE(\xi)_{gw}}{d \ln(f_r)}$  is the energy spectrum of a single GW event, which is calculated through the analysis of subsection 2, and  $f_r$  is the GW frequency in the rest frame of GW sources, and thus  $f_r = (1+z)f$ .

We mention that we denote the parameters related to the number density of GW sources collectively by  $\xi = \{\xi_1, \dots, \xi_m\}$ , and therefore  $\frac{dn}{d\xi_1 \dots d\xi_m dz} d\xi_1 \dots d\xi_m dz \equiv \frac{dn}{d\xi dz} d\xi dz$  is the number density of sources in the redshift interval  $[z, z + dz]$  and with source parameters in the interval  $[\xi, \xi + d\xi]$ . Hence, in the simple single event of two DM halos collision of the previous section we have  $\xi = \{M, x, v_\infty, b\}$ , where  $M = M_A + M_B$ ,  $x = M_A/M_B$ ,  $v_\infty = v_{A\infty} + v_{B\infty}$  and  $b = b_A + b_B$ .

Let us now calculate the full distribution function  $\frac{dn}{dz d\xi} = \frac{dn}{dz dM dx dv_\infty db}$ . As we have checked numerically, the variance of  $b, v_\infty$  has a minor effect on the final result, not affecting the order of magnitude. Hence, it is

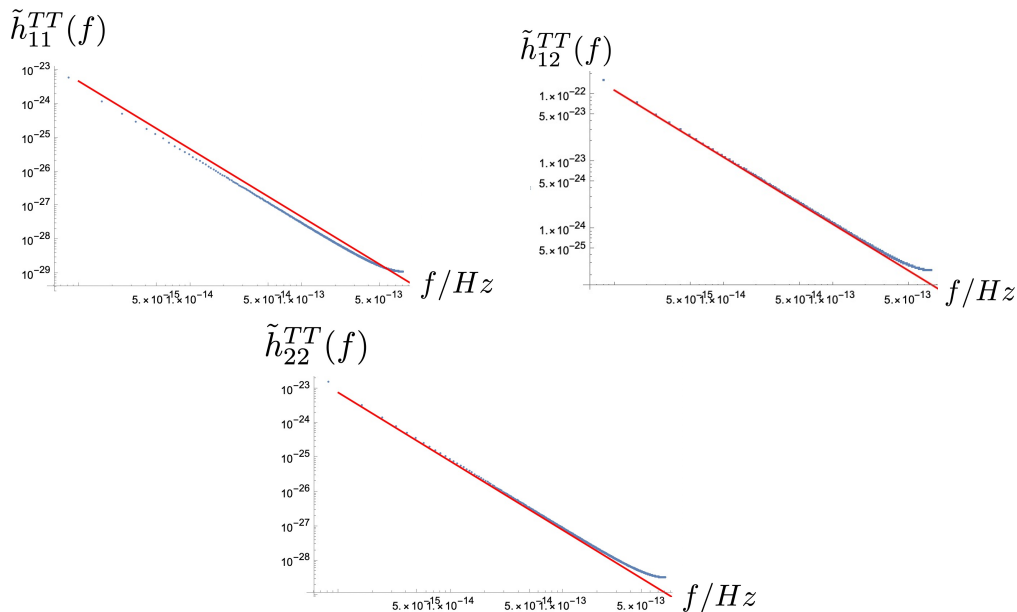


**Fig. 3** The spectrum of the gravitational waves as a function of the frequency. The upper left panel shows the  $\tilde{h}_{11}^{TT}(f)$  component, the upper right panel the  $\tilde{h}_{12}^{TT}(f)$  component and the lower center panel the  $\tilde{h}_{22}^{TT}(f)$  component. The blue dots represent the exact results at the time of shortest distance, while the red solid curves are power-law fits, specifically  $\tilde{h}_{11}^{TT}(f) \approx 4.7 \times 10^{-54} (Hz/f)^2$ ,  $\tilde{h}_{12}^{TT}(f) \approx 1.2 \times 10^{-38} (Hz/f)^2$ ,  $\tilde{h}_{22}^{TT}(f) \approx 7.7 \times 10^{-54} (Hz/f)^2$ .

a good approximation to omit the change of  $b, v_\infty$ , and consider that  $\xi = \{M, x\}$ . Hence, we have

$$\begin{aligned} \frac{d\rho_{\text{gw}}(f)}{d \ln f} &= \int_0^\infty dz \frac{1}{1+z} \int d\xi \frac{dn}{dz d\xi} \frac{dE(\xi)_{\text{gw}}}{d \ln f_r} \Big|_{f_r=f(1+z)} \\ &\approx \int_0^{10} dz \frac{1}{1+z} \int_{M_{\text{min}}=10^9 M_\odot}^{M_{\text{max}}=10^{15} M_\odot} dM \int_{x_{\text{min}}=1}^{x_{\text{max}}=10^5} dx \\ &\times \frac{dn}{dz dM dx} \frac{dE(\xi)_{\text{gw}}}{d \ln f_r} \Big|_{f_r=f(1+z)}, \end{aligned} \quad (38)$$

where the varying range of  $M$  and  $x$  is taken from [98].

In the following subsections we will separately calculate the energy spectrum of a single GW event  $\frac{dE(\xi)_{\text{gw}}}{d \ln f_r}$ , and the number density of GW sources  $\frac{dn}{dz dM dx}$ .

### 3.1 Energy spectrum of a single GW event

The energy density of a single GW event can be calculated from the (traceless) second time derivative of the quadrupole moment, namely [99]

$$\frac{dE(\xi)_{\text{gw}}}{d \ln f_r} \approx f_r \frac{2G}{5c^5} (2\pi f_r)^2 (\ddot{Q}_{ij}(M, x; f_r)) (\ddot{Q}_{ij}(M, x; f_r)), \quad (39)$$

where  $Q_{ij}$  is the traceless quadrupole moment and  $\ddot{Q}_{ij}$  is the Fourier transformation of the second time derivative

of  $Q_{ij}$ , which is related to  $I_{ij}$  via

$$Q_{11} = \frac{2}{3} I_{11} - \frac{1}{3} I_{22}, \quad (40)$$

$$Q_{22} = -\frac{1}{3} I_{11} + \frac{2}{3} I_{22}, \quad (41)$$

$$Q_{33} = -\frac{1}{3} I_{11} - \frac{1}{3} I_{22}, \quad (42)$$

$$Q_{21} = Q_{12} = I_{12}, \quad (43)$$

while all other  $Q_{ij}$  are equal to zero. Now, from Newtonian mechanics  $I_{ij}$  can be written as

$$\begin{aligned} \ddot{I}_{ij}(M, x; f_r) &= 4 \left[ \frac{x}{(1+x)^3} + \frac{1/x}{(1+1/x)^3} \right] \\ &\times \left( \frac{M}{2 \times 10^{12} M_\odot} \right)^2 \ddot{I}_{ij}^G(f_r), \end{aligned} \quad (44)$$

where  $x$  is the mass ratio of the two masses, and  $I_{ij}^G$  is defined as  $I_{ij}^G(M = 2 \times 10^{12} M_\odot, x = 1)$ . Therefore, from the calculation of Section 2, we can extract the values of  $\ddot{I}_{ij}^G(f_r)$  as

$$\ddot{I}_{11}^G(f_r) = 2.86 \times 10^{21} \left( \frac{\text{Hz}}{f_r} \right)^2 \text{ kg m}^2 \text{ s}^{-1}, \quad (45)$$

$$\ddot{I}_{22}^G(f_r) = 5.72 \times 10^{20} \left( \frac{\text{Hz}}{f_r} \right)^2 \text{ kg m}^2 \text{ s}^{-1}, \quad (46)$$

$$\ddot{I}_{12}^G(f_r) = \ddot{I}_{21}^G(f_r) = 1.29 \times 10^{37} \left( \frac{\text{Hz}}{f_r} \right) \text{ kg m}^2 \text{ s}^{-1}. \quad (47)$$

Hence, inserting the above into (39) gives us the energy density of a single GW event.

The energy density can be written as follows

$$\frac{dE(\xi)}{d\ln(f_r)} \propto M^2(C_1 f_r + C_2 \frac{1}{f_r}), \quad (48)$$

where  $C_1, C_2$  are constants. When  $f_r \geq 10^{-16} Hz$ , the contribution of  $\frac{1}{f_r}$  to the energy spectrum can be ignored. In this case, the energy spectrum is consistent with the result in [96] which is given by:

$$\frac{dE(\xi)}{d\ln(f_r)} \propto f_r M^2. \quad (49)$$

It should be noted that integrating the energy spectrum of gravitational waves over the entire frequency range to determine the total energy released throughout the process will result in divergence.

The physical process of releasing high-frequency gravitational waves corresponds to two particles being very close together, causing rapid changes in the motion of particles. At this point, the release of gravitational waves will in turn have a significant impact on the motion of the two particles, rendering the approximation of elastic collision ineffective. Further more, it would even be unreasonable to consider the collision of dark matter halos as point particles under such circumstances. Therefore, the frequency of the energy spectrum should be truncated at  $f_{max} \approx v/b$  in order to avoid non-physical results. For  $v \approx 300 km/s$  and  $b \approx 10^4 ly$ , the cutoff frequency  $f_{max} \approx 3.2 \times 10^{-15} Hz$ .

### 3.2 Number density of GW sources

Let us now calculate the number density of GW sources (per redshift, total mass and mass ratio interval)  $\frac{dn}{dzdMdx}$ . This number density is equal to the DM matter halos mergers rate, which can be calculated by combining the extended Press-Schechter (EPS) theory [96] and numerical simulations [98]:

$$\frac{dn}{dzdMdx} = n_{halo}(M, z) \frac{d\omega}{dz} \left( \frac{1}{n_{halo}} \frac{dn_{merger}}{d\omega dx} \right), \quad (50)$$

where  $n_{halo}(M, z)$  is the number density of dark matter halos (per redshift per mass interval in the co-moving space),  $\omega = \omega(z)$  is a redshift-dependent function given below, and  $(\frac{1}{n_{halo}} \frac{dn_{merger}}{d\omega dx})$  is the merger rate (at some  $\omega$ ) for a pair of DM halos with fixed total mass  $M$  and mass ratio  $x$ . In the following we handle these terms separately.

We start with the definition of  $\omega(z)$  [96]

$$\omega(z) = \frac{1.69}{D(z)}, \quad (51)$$

where  $D(z)$  is the linear growth rate of matter density.  $D(z)$  can be written as

$$D(z) = \frac{1}{g(z=0)} \left[ \frac{g(z)}{1+z} \right], \quad (52)$$

where a good approximation of  $g(z)$  is

$$g(z) \approx \frac{5}{2} \Omega_m(z) \times \left\{ \Omega_m^{4/7}(z) - \Omega_\Lambda(z) + [1 + \Omega_m(z)/2][1 + \Omega_\Lambda(z)/70] \right\}^{-1}, \quad (53)$$

with  $\Omega_\Lambda(z)$ ,  $\Omega_m(z)$  the density parameters of dark energy and matter sectors given by

$$\Omega_\Lambda(z) = \frac{\Omega_{\Lambda,0}}{E^2(z)}; \quad \Omega_m(z) = \frac{\Omega_{m,0}(1+z)^3}{E^2(z)}, \quad (54)$$

where the normalized Hubble function  $E(z) \equiv H(z)/H_0$  reads as

$$E(z) \approx [\Omega_{\Lambda,0} + \Omega_{m,0}(1+z)^3]^{1/2}, \quad (55)$$

with the value of the Hubble function at present time given as [70]

$$H_0 \approx 67.3 km s^{-1} Mpc^{-1}, \quad (56)$$

and with the values  $\Omega_{\Lambda,0}, \Omega_{m,0}$  at present time taken as [70]

$$\Omega_{\Lambda,0} \approx 0.685, \quad (57)$$

$$\Omega_{m,0} \approx 0.317. \quad (58)$$

Note that in the above we consider that the underlying cosmology is  $\Lambda$ CDM concordance scenario, i.e., the dark energy sector is the cosmological constant.

We continue by using the EPS theory in order to write the formula of the number density of DM halos  $n_{halo}$ . We consider that the halos merge when the redshift is between  $z$  and  $z + dz$ , and that the emitted GW signals are detected at Earth at present. In co-moving space those halos are in the volume  $\Delta V = 4\pi r^2(z) dr(z)$ . Now, the EPS theory provides the number density of DM halos  $n_{EPS}(M, z)$  at some redshift  $z$  and mass  $M$ . Therefore, we have

$$n_{halo} = 4\pi r^2(z) \frac{dr(z)}{dz} n_{EPS}(M, z), \quad (59)$$

where the radius in the co-moving space  $r(z)$  is [96]

$$r(z) = \frac{c}{H_0} \int_0^z dz' \frac{1}{E(z')}, \quad (60)$$

while the formula of  $n_{EPS}(M, z)$  is [96]

$$n_{EPS}(M, z) = \sqrt{\frac{2}{\pi}} \frac{\bar{\rho}}{M^2} \frac{\delta_c}{\sigma} \exp\left(-\frac{\delta_c^2}{2\sigma^2}\right) \left| \frac{d\ln \sigma}{d\ln M} \right|. \quad (61)$$

In the above expression  $\bar{\rho} = \rho_c \Omega_{m,0}$  is the mean density of the matter component,  $\delta_c = \omega = \frac{1.69}{D(z)}$ , while  $\sigma(M)$  is the variance of the matter density perturbation which can be estimated as [96]

$$\sigma(M) \approx \sigma_8 \left( \frac{R}{r_8} \right)^{-\beta}, \quad (62)$$

with  $M = \frac{4\pi}{3} \bar{\rho} R^3$ ,  $\sigma_8 \approx 1$ ,  $\beta \approx 0.6 + 0.8(\Omega_{m,0} h)$ ,  $h = 0.673$ , and  $r_8 = 8 \text{ Mpc } h^{-1}$ , leading to

$$\left| \frac{d \ln \sigma}{d \ln M} \right| = \frac{\beta}{3}. \quad (63)$$

Finally, the last term of (50), namely  $\left( \frac{1}{n_{\text{halo}}} \frac{dn_{\text{merger}}}{d\omega dx} \right)$  (dimensionless since both  $\omega, x$  are dimensionless), can be found in [98] and it is given by

$$\left( \frac{1}{n_{\text{halo}}} \frac{dn_{\text{merger}}}{d\omega dx} \right) = A \left( \frac{M}{10^{12} M_{\odot}} \right)^{\alpha} x^b \exp[(\tilde{x}/x)^{\gamma}], \quad (64)$$

where the best-fit parameters from simulations are  $A = 0.065$ ,  $\alpha = 0.15$ ,  $b = -0.3$ ,  $\tilde{x} = 2.5$ ,  $\gamma = 0.5$  [98].

In summary, inserting (51), (59) and (64) into (50), provides the value of the number density of GW sources  $\frac{dn}{dz dM dx}$ .

### 3.3 The energy spectrum of the stochastic gravitational wave background

We have now all the ingredients needed in order to calculate the energy spectrum of the stochastic gravitational wave background. This is given by (38), in which the energy spectrum of a single GW event  $\frac{dE(\xi)_{\text{gw}}}{d \ln f_r}$  was calculated in subsection 3.1, while the number density of GW sources  $\frac{dn}{dz dM dx}$  was calculated in subsection 3.2. Assembling everything, we finally obtain the stochastic gravitational wave background resulting from DM halos collisions in the universe, which is calculated numerically and it is shown in Fig. 4. Besides, instantaneous collision approximation introduce a cutoff frequency, the frequency beyond which the signal is truncated is the inverse of the timescale of the collision. The cutoff frequency for instantaneous collisions is  $f_{\text{max}} \approx v/b$ . For the case of the dark matter halos collisions, This frequency is about  $3 \times 10^{-15} \text{ Hz}$ .

As we can see, the contribution of GW radiated from the collisions of DM halos, namely galaxies and galaxy clusters, is quite small comparing to other sources. In the pulsar timing array (PTA) band, where  $f \approx 10^{-9} \text{ Hz}$ , and where the current observational limit is  $h_c \approx 10^{-15}$  [100]. we obtain an effect of the order of  $h_c \approx 10^{-29}$  in the band of  $f \approx 10^{-15} \text{ Hz}$ . Nevertheless, in very

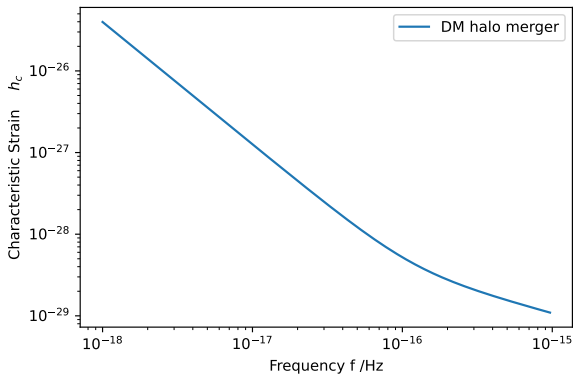


**Fig. 4** The characteristic strain  $h_c(f)$  as a function of the frequency of the stochastic gravitational wave background created by DM halos, namely galaxies and galaxy clusters, collisions .

low frequency band  $h_c$  will be larger. In general, with current observational sensitivity the effect of the DM halos collisions on the stochastic gravitational wave background cannot be detected [101, 102, 103, 104]. Note that one could try to extend the analysis, by considering, instead of point masses, a group of mass points with Navarro, Frenk & White (NFW) density profile [96] to simulate DM halo collisions, nevertheless the results are expected to be at the same order of magnitude.

Dark matter halos are in reality extended objects and not point-particles. Strictly speaking, this two point toy model only suits for the beginning of the merger of 2 DM halos, at this stage the mechanical energy of the 2 mass centers of DM halo is approximately a constant. One may use N-body simulation to calculate the GW radiated from the merger more precisely. However, as an estimation of order of magnitude of the contribution to the GWB, the simple model in this paper is good enough.

## 4 Conclusions

In this work we investigated the effect of the dark matter halos collisions, namely collisions of galaxies and galaxy clusters, through gravitational bremsstrahlung, on the stochastic gravitational wave background.

In order to achieve this goal, we first calculated the gravitational wave signal of a single DM halo collision event. As an estimation of the order of magnitude, we handled the two DM halos as mass points. Furthermore, since the strength of such GW signals is weak, we adopted linear perturbation theory of General Relativity, namely we extracted the GW signal using the second time derivative of the quadrupole moment. Additionally, since the velocity of DM halos is small, we



applied non-relativistic Newtonian Mechanics. Hence, we extracted the GW signal through bremsstrahlung from a single DM halo collision. As we showed,  $\bar{h}_{ij}$  is of the order of  $10^{-22}$ , and it becomes maximum at the time of shortest distance as expected. However, since such an event typically corresponds to duration of the order of  $10^{15}s$ , we deduce that a single signal of this kind of GW is extremely hard to be detected.

As a next step we proceeded to the calculation of the energy spectrum of the collective effect of all DM halos collisions in the Universe. This can arise by the energy spectrum of a GW signal radiated by a single collision, multiplied by the DM halo collision rate, and integrating over the whole Universe. Firstly, knowing the signal of a single collision we calculated its energy spectrum. Secondly, concerning the DM halo collision rate we showed that it is given by the product of the number density of DM halos, which is calculated by the EPS theory, with the collision rate of a single DM halo, which is given by simulation results, with a function of the linear growth rate of matter density through cosmological evolution. Hence, integrating over all mass and distance ranges, we finally extracted the spectrum of the stochastic gravitational wave background created by DM halos collisions.

As we show, the resulting contribution to the stochastic gravitational wave background is of the order of  $h_c \approx 10^{-29}$  in the band of  $f \approx 10^{-15}Hz$ . However, in very low frequency band,  $h_c$  is larger. With current observational sensitivity it cannot be detected.

In summary, with the current and future significant advance in gravitational-wave astronomy, and in particular with the tremendous improvement on the sensitivity bounds that Collaborations like Laser Interferometer Space Antenna (LISA), Einstein Telescope (ET), Cosmic Explorer (CE), etc will bring, it is both interesting and necessary to investigate all possible contributions to the stochastic gravitational wave background. And the gravitational bremsstrahlung during galaxies and galaxy clusters collisions is one of them.

## Acknowledgments

We are grateful to Yifu Cai, Jiewen Chen, Zihan Zhou, Jiarui Li and Yumin Hu, Bo Wang and Rui Niu for helpful discussions. This work is supported in part by the National Key R&D Program of China (2021YFC2203100), by CAS young interdisciplinary innovation team (JCTD-2022-20), by the NSFC (12261131497), by 111 Project for ‘‘Observational and Theoretical Research on Dark Matter and Dark Energy’’ (B23042), by the Fundamental Research Funds for Central Universities, by the CSC Innovation Talent Funds, by the USTC Fellowship

for International Cooperation, and by the USTC Research Funds of the Double First-Class Initiative. ENS acknowledges participation in the COST Association Action CA18108 ‘‘Quantum Gravity Phenomenology in the Multimessenger Approach (QG-MM)’’. All numerics were operated on the computer clusters *LINDA* & *JUDY* in the particle cosmology group at USTC.

## References

1. B.P. Abbott, et al., Phys. Rev. Lett. **116**(6), 061102 (2016). DOI 10.1103/PhysRevLett.116.061102
2. B.P. Abbott, et al., Phys. Rev. Lett. **119**(16), 161101 (2017). DOI 10.1103/PhysRevLett.119.161101
3. A. Goldstein, et al., Astrophys. J. Lett. **848**(2), L14 (2017). DOI 10.3847/2041-8213/aa8f41
4. A. Addazi, et al., Prog. Part. Nucl. Phys. **125**, 103948 (2022). DOI 10.1016/j.pnpnp.2022.103948
5. R. Abbott, et al., Phys. Rev. X **11**, 021053 (2021). DOI 10.1103/PhysRevX.11.021053
6. J.M. Ezquiaga, M. Zumalacárregui, Phys. Rev. Lett. **119**(25), 251304 (2017). DOI 10.1103/PhysRevLett.119.251304
7. W. Zhao, L. Wen, Phys. Rev. D **97**(6), 064031 (2018). DOI 10.1103/PhysRevD.97.064031
8. B.P. Abbott, et al., Astrophys. J. Lett. **848**(2), L13 (2017). DOI 10.3847/2041-8213/aa920c
9. B.P. Abbott, et al., Nature **551**(7678), 85 (2017). DOI 10.1038/nature24471
10. T. Baker, E. Bellini, P.G. Ferreira, M. Lagos, J. Noller, I. Sawicki, Phys. Rev. Lett. **119**(25), 251301 (2017). DOI 10.1103/PhysRevLett.119.251301
11. G. Farrugia, J. Levi Said, V. Gakis, E.N. Saridakis, Phys. Rev. D **97**(12), 124064 (2018). DOI 10.1103/PhysRevD.97.124064
12. Y.F. Cai, C. Li, E.N. Saridakis, L. Xue, Phys. Rev. D **97**(10), 103513 (2018). DOI 10.1103/PhysRevD.97.103513
13. M. Hohmann, C. Pfeifer, J. Levi Said, U. Ualikhanova, Phys. Rev. D **99**(2), 024009 (2019). DOI 10.1103/PhysRevD.99.024009
14. E.N. Saridakis, et al., (2021)
15. P. Amaro-Seoane, et al., Class. Quant. Grav. **29**, 124016 (2012). DOI 10.1088/0264-9381/29/12/124016
16. P. Amaro-Seoane, et al., (2017)
17. T. Papanikolaou, JCAP **10**, 089 (2022). DOI 10.1088/1475-7516/2022/10/089
18. G. Domènech, C. Lin, M. Sasaki, JCAP **04**, 062 (2021). DOI 10.1088/1475-7516/2021/11/E01. [Erratum: JCAP **11**, E01 (2021)]
19. L. Lentati, et al., Mon. Not. Roy. Astron. Soc. **453**(3), 2576 (2015). DOI 10.1093/mnras/stv1538
20. Z. Arzoumanian, et al., Astrophys. J. Lett. **905**(2), L34 (2020). DOI 10.3847/2041-8213/abd401
21. J.W. Chen, Y. Wang, Astrophys. J. **929**(2), 168 (2022). DOI 10.3847/1538-4357/ac5bd4
22. J.W. Chen, Y. Zhang, Mon. Not. Roy. Astron. Soc. **481**(2), 2249 (2018). DOI 10.1093/mnras/sty2268
23. J. Antoniadis, et al., Astron. Astrophys. **678**, A48 (2023). DOI 10.1051/0004-6361/202346841
24. J. Antoniadis, et al., (2023)
25. N. Christensen, Rept. Prog. Phys. **82**(1), 016903 (2019). DOI 10.1088/1361-6633/aae6b5

26. B.P. Abbott, et al., *Phys. Rev. Lett.* **116**(13), 131102 (2016). DOI 10.1103/PhysRevLett.116.131102
27. B.J. Owen, L. Lindblom, C. Cutler, B.F. Schutz, A. Vecchio, N. Andersson, *Phys. Rev. D* **58**, 084020 (1998). DOI 10.1103/PhysRevD.58.084020
28. A.H. Jaffe, D.C. Backer, *Astrophys. J.* **583**, 616 (2003). DOI 10.1086/345443
29. N. Stergioulas, A. Bauswein, K. Zagkouris, H.T. Janka, *Mon. Not. Roy. Astron. Soc.* **418**, 427 (2011). DOI 10.1111/j.1365-2966.2011.19493.x
30. J.A. Clark, A. Bauswein, N. Stergioulas, D. Shoemaker, *Class. Quant. Grav.* **33**(8), 085003 (2016). DOI 10.1088/0264-9381/33/8/085003
31. F. De Lillo, J. Suresh, A.L. Miller, *Mon. Not. Roy. Astron. Soc.* **513**(1), 1105 (2022). DOI 10.1093/mnras/stac984
32. D. Agarwal, J. Suresh, V. Mandic, A. Matas, T. Regimbau, *Phys. Rev. D* **106**(4), 043019 (2022). DOI 10.1103/PhysRevD.106.043019
33. Y.T. Wang, Y. Cai, Z.G. Liu, Y.S. Piao, *JCAP* **01**, 010 (2017). DOI 10.1088/1475-7516/2017/01/010
34. R. Flauger, N. Karnesis, G. Nardini, M. Pieroni, A. Ricciardone, J. Torrado, *JCAP* **01**, 059 (2021). DOI 10.1088/1475-7516/2021/01/059
35. N. Bellomo, D. Bertacca, A.C. Jenkins, S. Matarrese, A. Raccanelli, T. Regimbau, A. Ricciardone, M. Sakellariadou, *JCAP* **06**(06), 030 (2022). DOI 10.1088/1475-7516/2022/06/030
36. Z. Zhao, Y. Di, L. Bian, R.G. Cai, (2022)
37. M. Maggiore, *Phys. Rept.* **331**, 283 (2000). DOI 10.1016/S0370-1573(99)00102-7
38. K.N. Ananda, C. Clarkson, D. Wands, *Phys. Rev. D* **75**, 123518 (2007). DOI 10.1103/PhysRevD.75.123518
39. C. Caprini, D.G. Figueroa, *Class. Quant. Grav.* **35**(16), 163001 (2018). DOI 10.1088/1361-6382/aac608
40. I. Musco, J.C. Miller, *Class. Quant. Grav.* **30**, 145009 (2013). DOI 10.1088/0264-9381/30/14/145009
41. T. Papanikolaou, C. Tzerefos, S. Basilakos, E.N. Saridakis, *JCAP* **10**, 013 (2022). DOI 10.1088/1475-7516/2022/10/013
42. T. Papanikolaou, C. Tzerefos, S. Basilakos, E.N. Saridakis, *Eur. Phys. J. C* **83**(1), 31 (2023). DOI 10.1140/epjc/s10052-022-11157-4
43. S. Banerjee, T. Papanikolaou, E.N. Saridakis, *Phys. Rev. D* **106**(12), 124012 (2022). DOI 10.1103/PhysRevD.106.124012
44. T. Papanikolaou, V. Vennin, D. Langlois, *JCAP* **03**, 053 (2021). DOI 10.1088/1475-7516/2021/03/053
45. J.F. Dufaux, A. Bergman, G.N. Felder, L. Kofman, J.P. Uzan, *Phys. Rev. D* **76**, 123517 (2007). DOI 10.1103/PhysRevD.76.123517
46. Y.f. Cai, Y.S. Piao, *Phys. Lett. B* **657**, 1 (2007). DOI 10.1016/j.physletb.2007.09.068
47. S. Kuroyanagi, T. Chiba, N. Sugiyama, *Phys. Rev. D* **79**, 103501 (2009). DOI 10.1103/PhysRevD.79.103501
48. N.E. Mavromatos, J. Solà Peracaula, *Eur. Phys. J. ST* **230**(9), 2077 (2021). DOI 10.1140/epjs/s11734-021-00197-8
49. Z. Zhou, J. Jiang, Y.F. Cai, M. Sasaki, S. Pi, *Phys. Rev. D* **102**(10), 103527 (2020). DOI 10.1103/PhysRevD.102.103527
50. A. Achúcarro, et al., (2022)
51. M. Zhu, A. Ilyas, Y. Zheng, Y.F. Cai, E.N. Saridakis, *JCAP* **11**(11), 045 (2021). DOI 10.1088/1475-7516/2021/11/045
52. Y.F. Cai, X.H. Ma, M. Sasaki, D.G. Wang, Z. Zhou, *JCAP* **12**, 034 (2022). DOI 10.1088/1475-7516/2022/12/034
53. G. Franciolini, I. Musco, P. Pani, A. Urbano, *Phys. Rev. D* **106**(12), 123526 (2022). DOI 10.1103/PhysRevD.106.123526
54. A. Addazi, S. Capozziello, Q. Gan, *JCAP* **08**(08), 051 (2022). DOI 10.1088/1475-7516/2022/08/051
55. N.E. Mavromatos, V.C. Spanos, I.D. Stamou, *Phys. Rev. D* **106**(6), 063532 (2022). DOI 10.1103/PhysRevD.106.063532
56. S. Kazempour, A.R. Akbarieh, E.N. Saridakis, *Phys. Rev. D* **106**(10), 103502 (2022). DOI 10.1103/PhysRevD.106.103502
57. T. Papanikolaou, A. Lymperis, S. Lola, E.N. Saridakis, *JCAP* **03**, 003 (2023). DOI 10.1088/1475-7516/2023/03/003
58. B. Allen, J.D. Romano, *Phys. Rev. D* **59**, 102001 (1999). DOI 10.1103/PhysRevD.59.102001
59. S. Capozziello, M. De Laurentis, S. Nojiri, S.D. Odintsov, *Gen. Rel. Grav.* **41**, 2313 (2009). DOI 10.1007/s10714-009-0758-1
60. A. Sesana, A. Vecchio, C.N. Colacino, *Mon. Not. Roy. Astron. Soc.* **390**, 192 (2008). DOI 10.1111/j.1365-2966.2008.13682.x
61. J.D. Romano, N.J. Cornish, *Living Rev. Rel.* **20**(1), 2 (2017). DOI 10.1007/s41114-017-0004-1
62. P. Huang, A.J. Long, L.T. Wang, *Phys. Rev. D* **94**(7), 075008 (2016). DOI 10.1103/PhysRevD.94.075008
63. R.G. Cai, T.B. Liu, X.W. Liu, S.J. Wang, T. Yang, *Phys. Rev. D* **97**(10), 103005 (2018). DOI 10.1103/PhysRevD.97.103005
64. Y.F. Cai, C. Chen, X. Tong, D.G. Wang, S.F. Yan, *Phys. Rev. D* **100**(4), 043518 (2019). DOI 10.1103/PhysRevD.100.043518
65. T. Regimbau, *Symmetry* **14**(2), 270 (2022). DOI 10.3390/sym14020270
66. Z. Arzoumanian, et al., *Astrophys. J.* **859**(1), 47 (2018). DOI 10.3847/1538-4357/aabd3b
67. L. Speri, N. Karnesis, A.I. Renzini, J.R. Gair, *Nature Astron.* **6**(12), 1356 (2022). DOI 10.1038/s41550-022-01849-y
68. M. Georgousi, N. Karnesis, V. Korol, M. Pieroni, N. Stergioulas, *Mon. Not. Roy. Astron. Soc.* **519**(2), 2552 (2022). DOI 10.1093/mnras/stac3686
69. G. Agazie, et al., *Astrophys. J. Lett.* **952**(2), L37 (2023). DOI 10.3847/2041-8213/ace18b
70. N. Aghanim, et al., *Astron. Astrophys.* **641**, A1 (2020). DOI 10.1051/0004-6361/201833880
71. N. Aghanim, et al., *Astron. Astrophys.* **641**, A6 (2020). DOI 10.1051/0004-6361/201833910. [Erratum: *Astron. Astrophys.* 652, C4 (2021)]
72. P.A.R. Ade, et al., *Astron. Astrophys.* **571**, A16 (2014). DOI 10.1051/0004-6361/201321591
73. G. Bertone, D. Hooper, J. Silk, *Phys. Rept.* **405**, 279 (2005). DOI 10.1016/j.physrep.2004.08.031
74. G. Jungman, M. Kamionkowski, K. Griest, *Phys. Rept.* **267**, 195 (1996). DOI 10.1016/0370-1573(95)00058-5
75. J. Preskill, M.B. Wise, F. Wilczek, *Phys. Lett. B* **120**, 127 (1983). DOI 10.1016/0370-2693(83)90637-8
76. N. Arkani-Hamed, D.P. Finkbeiner, T.R. Slatyer, N. Weiner, *Phys. Rev. D* **79**, 015014 (2009). DOI 10.1103/PhysRevD.79.015014
77. V.C. Rubin, N. Thonnard, W.K. Ford, Jr., *Astrophys. J.* **238**, 471 (1980). DOI 10.1086/158003
78. D. Clowe, M. Bradac, A.H. Gonzalez, M. Markevitch, S.W. Randall, C. Jones, D. Zaritsky, *Astrophys. J. Lett.* **648**, L109 (2006). DOI 10.1086/508162
79. J.F. Navarro, C.S. Frenk, S.D.M. White, *Astrophys. J.* **462**, 563 (1996). DOI 10.1086/177173

- 
80. M. Davis, G. Efstathiou, C.S. Frenk, S.D.M. White, *Astrophys. J.* **292**, 371 (1985). DOI 10.1086/163168
  81. S.D.M. White, M.J. Rees, *Mon. Not. Roy. Astron. Soc.* **183**, 341 (1978). DOI 10.1093/mnras/183.3.341
  82. J.S. Bullock, T.S. Kolatt, Y. Sigad, R.S. Somerville, A.V. Kravtsov, A.A. Klypin, J.R. Primack, A. Dekel, *Mon. Not. Roy. Astron. Soc.* **321**, 559 (2001). DOI 10.1046/j.1365-8711.2001.04068.x
  83. P.C. Peters, *Phys. Rev. D* **1**, 1559 (1970). DOI 10.1103/PhysRevD.1.1559
  84. R.J. Crowley, K.S. Thorne, *Astrophys. J.* **215**, 624 (1977). DOI 10.1086/155397
  85. L. Smarr, *Phys. Rev. D* **15**, 2069 (1977). DOI 10.1103/PhysRevD.15.2069
  86. S.J. Kovacs, K.S. Thorne, *Astrophys. J.* **224**, 62 (1978). DOI 10.1086/156350
  87. B.D. Farris, Y.T. Liu, S.L. Shapiro, *Phys. Rev. D* **84**, 024024 (2011). DOI 10.1103/PhysRevD.84.024024
  88. S. Moushiakakos, M.M. Riva, F. Vernizzi, *Phys. Rev. D* **104**(2), 024041 (2021). DOI 10.1103/PhysRevD.104.024041
  89. E. Herrmann, J. Parra-Martinez, M.S. Ruf, M. Zeng, *Phys. Rev. Lett.* **126**(20), 201602 (2021). DOI 10.1103/PhysRevLett.126.201602
  90. S. Moushiakakos, M.M. Riva, F. Vernizzi, *Phys. Rev. Lett.* **129**(12), 121101 (2022). DOI 10.1103/PhysRevLett.129.121101
  91. G.U. Jakobsen, G. Mogull, J. Plefka, J. Steinhoff, *Phys. Rev. Lett.* **128**(1), 011101 (2022). DOI 10.1103/PhysRevLett.128.011101
  92. L. Gondán, B. Kocsis, *Mon. Not. Roy. Astron. Soc.* **515**(3), 3299 (2022). DOI 10.1093/mnras/stac1985
  93. M.M. Riva, F. Vernizzi, L.K. Wong, *Phys. Rev. D* **106**(4), 044013 (2022). DOI 10.1103/PhysRevD.106.044013
  94. T. Inagaki, K. Takahashi, S. Masaki, N. Sugiyama, *Phys. Rev. D* **82**, 124007 (2010). DOI 10.1103/PhysRevD.82.124007
  95. T. Inagaki, K. Takahashi, N. Sugiyama, *Phys. Rev. D* **85**, 104051 (2012). DOI 10.1103/PhysRevD.85.104051
  96. H. Mo, F.C. van den Bosch, S. White, *Galaxy Formation and Evolution* (2010)
  97. M. Maggiore, *Gravitational Waves. Vol. 1: Theory and Experiments*. Oxford Master Series in Physics (Oxford University Press, 2007)
  98. S. Genel, N. Bouche, T. Naab, A. Sternberg, R. Genzel, *Astrophys. J.* **719**, 229 (2010). DOI 10.1088/0004-637X/719/1/229
  99. M. Maggiore, *Gravitational Waves. Vol. 2: Astrophysics and Cosmology* (Oxford University Press, 2018)
  100. S. Burke-Spolaor, et al., *Astron. Astrophys. Rev.* **27**(1), 5 (2019). DOI 10.1007/s00159-019-0115-7
  101. M. Tinto, J.W. Armstrong, F.B. Estabrook, *Phys. Rev. D* **63**, 021101 (2001). DOI 10.1103/PhysRevD.63.021101
  102. C. Caprini, D.G. Figueroa, R. Flauger, G. Nardini, M. Peloso, M. Pieroni, A. Ricciardone, G. Tasinato, *JCAP* **11**, 017 (2019). DOI 10.1088/1475-7516/2019/11/017
  103. N. Karnesis, et al., (2022)
  104. C.E.A. Chapman-Bird, C.P.L. Berry, G. Woan, *Mon. Not. Roy. Astron. Soc.* **522**(4), 6043 (2023). DOI 10.1093/mnras/stad1397